Accepted Manuscript

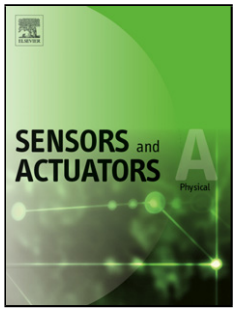

Title: A Flexible Tube-Based Triboelectric- Electromagnetic Sensor for Knee Rehabilitation Assessment

Author: Hassan Askari Ehsan Asadi Zia Saadatnia Amir Khajepour Mir Behrad Khamesee Jean Zu

PII: S0924-4247(17)32086-1
DOI: https://doi.org/doi:10.1016/j.sna.2018.05.016
Reference: SNA 10777

To appear in: *Sensors and Actuators A*

Received date: 17-11-2017
Revised date: 7-5-2018
Accepted date: 8-5-2018

Please cite this article as: Hassan Askari, Ehsan Asadi, Zia Saadatnia, Amir Khajepour, Mir Behrad Khamesee, Jean Zu, A Flexible Tube-Based Triboelectric- Electromagnetic Sensor for Knee Rehabilitation Assessment, *<![CDATA[Sensors & Actuators: A. Physical]]>* (2018), https://doi.org/10.1016/j.sna.2018.05.016

A Flexible Tube-Based Triboelectric- Electromagnetic Sensor for Knee Rehabilitation Assessment

Hassan Askari[a,*], Ehsan Asadi[a], Zia Saadatnia[b], Amir Khajepour[a], Mir Behrad Khamesee[a], Jean Zu[b]

[a] *Department of Mechanical and Mechatronics Engineering, University of Waterloo, 200 University Ave. West, Waterloo, ON N2L 3G1, Canada*

[b] *Department of Mechanical and Industrial Engineering, University of Toronto, Toronto, ON, M5S 3G8, Canada*

Abstract

This paper reports a novel hybridized flexible electromagnetic-triboelectric generator for vibration/deflection monitoring as it is implemented in a cantilever or clamped-clamped configuration.The proposed self-powered sensor operates based on the concepts of electromagnetism and triboelectricity. The fabricated device consists of a stack of magnets and coils, a flexible tube as the main body, and also, highly flexible, mechanically and thermally durable, and cost-effective polymeric materials.The configuration of the electromagnetic component is optimized based on the magnetization direction of the utilized magnets. The device can effectively convert the shear force and bending moment to electrical voltage through the hybridized system with exerting an external force. The performance of the self-powered sensor is investigated for different cases including a single stack and also a double stack of magnetic components. The design of the triboelectric component of the device is based on the vertical contact separation mode. Results of the paper show how the change of configuration of the magnetic components alters the electrical output of the sensor. A detailed experimental analysis is provided to show the capability of the device under different excitation conditions for both TENG and EMG components of the sensor.As the experimental analysis shows, the proposed self-powered system has the potential to be utilized for knee rehabilitation, as it shows explicit results under periodical bending load with different frequencies and amplitudes of excitation.

Keywords: Hybridized nano generator, Electromagnetism, Triboelectricity, Self-powered sensor, Knee rehabilitation.

*Corresponding Author

Email addresses: h2askari@uwaterloo.ca (Hassan Askari), easadi@uwaterloo.ca (Ehsan Asadi), zsaadat@mie.utoronto.ca (Zia Saadatnia), akhajepour@uwaterloo.ca (Amir Khajepour), khamesee@uwaterloo.ca (Mir Behrad Khamesee), zu@mie.utoronto.ca (Jean Zu)

1. INTRODUCTION

Nowadays, developing new type of self-powered sensors is a growing and intriguing area of research due to substantial technological advancement in mobile devices and increasing demand of portable or wearable electronics. Self-powered sensors technology is maturing rapidly, and it is a momentous step towards future smart cities and tremendously beneficial for improving our quality of life. As the size of the portable and wearable electronics decreases over the time, lower rates of power is required to operate those devices. Therefore, it is feasible to operate the small-size electronics entirely by scavenging ambient energy. A tremendous amount of researches conducted by scientists, in this area, where the ultimate goal is to find alternative power sources for electronics. Such achievement enables us to remove the need to A: replace battery in battery operated electronics, and B: utilize miniature sensing devices in remote locations. Knee rehabilitation assessment and tire pressure monitoring are two prominent examples for the above mentioned A and B goals, respectively.

Exploration of researchers in this area has resulted in four main techniques for energy harvesting: electrostatic[1, 2], piezoelectric [3, 4], electromagnetic[5, 6], and triboelectric energy harvesting [7–15]. Combination of EMG and TENG in a singular package provides many advantages including a broadband range of frequency operation as well as high sensitivity to small excitation amplitudes [16–18]. The advantages of hybridization have prompted researchers to exploit it for plenty of different applications including ocean wave [19] and wind energy harvesting, self-powered watch, traffic monitoring[20], and scavenging bio-mechanical energy[21].

Recently, triboelectricity has emerged as a potent platform for both energy harvesting and self-powered sensing. The term triboelectric effect has come to be used to refer to the electrically charging process when two different materials contact each other through friction[16, 22–24]. Utilization of this effect results in an electric potential based on the opposite charges on both friction surfaces. The relative motion of contact layers lead to flow of electron through an external circuit [25–28]. In accordance with this phenomenon, four different modes of TENGs have been invented including vertical contact-separation [29–33], lateral sliding [21, 24, 34–37], single electrode[38–41], and freestanding modes [42, 43].In our proposed sensory device, we use vertical contact separation mode with single electrode. Vertical contact-separation (VCS) is one of the most utilized modes by researchers in this area. As one of the earliest endeavors of using VCS, Wang et al. [44] fabricated an arch-shaped VCS-TENG with application in powering portable electronic devices. Zhu et al. developed a TENG-based sensor which is capable of generating instantaneous power of 31.2 $\frac{mW}{cm^3}$ with maximum output voltage of 110 V[45]. Cheng et al. [46] developed a pulsed based VCS-TENGs nano generator, where the instantaneous output power is hugely improved by reducing the duration of the charging/discharge process utilizing 'off-on-off' contact based switching. He et al. increased the energy conversion efficiency of the VCS-TENG by mixing suitable amount of conductive nanoparticles into the polymer, which results in increasing the charge density on the polymer surface. Their technique enhances the output power of TENG about 2.6 times comparing to the pure polymer film[47].

One of the main applications of VCS-TENGs is in wave and wind energy harvesting[48].

Plenty of key steps have been taken in this area by Wangs group in Georgia Tech[49]. For example, Bae et al. employed VCS-TENGs for harvesting wind energy based on flutter-driven triboelectrification and were able to reach an instantaneous output voltage of 200 V and a current of 60 mA with a high frequency of 158 Hz, and with an average power density of 0.86 mW [50]. In a ground-breaking work, Chen et al. [51] proposed the possible use of a network of TENG for water wave energy harvesting with the potential to scavenge 1.15 MW from 1 km^2 surface area. Considering the light-weight, cost effective, environmentally friendly, and simple implementation of a network of TENG in ocean, this type of energy harvesting has a momentous potential towards blue energy harvesting from the ocean.

Another aspect of utilizing VCS-TENG is in pressure sensing. In a seminal and important study, Fan et al. reported a transparent self-powered pressure sensor highly applicable in organic electronic and optoelectronic devices. Their as-fabricated self-powered sensor is significantly sensitive to very small pressure and can detect a water droplet and a falling feather[52]. Also, Dhakar et al.[53] developed large Scale self-powered pressure sensor array using roll-to-roll ultraviolet embossing to pattern polyethylene terephthalate sheets. Lee et al. [54] developed a fully packaged self-powered pressure sensor with hemispheres array. Their fabricated self-powered sensor is capable of generating 2.45 μW at load resistance of 3 $M\Omega$.

VCS-TENGs have been also used for energy harvesting from human motion and self-powered bio-medical systems[55, 56]. For instance, Tang et al. reported a self-powered low level laser cure system for osteogenesis exploiting TENGs. They identified that the system significantly accelerated the mouse embryonic osteoblasts proliferation and differentiation[57]. VCS-TENGs have shown promising potential for developing future smart keyboards. For example, Li et al.[58] reported an elastomer-based TENG as a keyboard cover. They showed that typing with the fabricated keyboard with normal speed for 1 h can generate $8 \times 10^{-4} J$ electricity, which can be used for driving an electronic thermometer/hydrometer. Recently, Ahmad et al. [59] developed a washable, stretchable, and self-powered human-machine interfacing self-powered sensor based on VCS-TENG. They concluded that the proposed system can charge a 10 μF capacitor up to 2.5V with the maximum power of 0.3 μW. The interesting result of the work is its capability for detecting of different users' typing pattern, which is a crucial factor for security system in computers.

Research into electromagnet power generators has a long history. According to the Faraday's ground breaking scientific work, any electromagnetic harvester consists of at least one coil and one magnet, and also a relative motion is necessary between them to generate voltage, and thus, to induce current flow in the coil. The low cost, feasibility and practicability of the electromagnetic mechanism have fascinated researchers to implement them for energy harvesting from different sources.

The present research reports a flexible self-powered sensor to address the growing demands for vibration, motion and deflection monitoring devices. The proposed self-powered sensor has hybridized design, and works in accordance with the concepts of electromagnetism and triboelectricty. The designed configuration includes one flexible tube with the electromagnetic and triboelectric components being implemented inside the tube and on the outer surface of the tube, respectively. Owning to the highly flexible design and self-

powered nature of the proposed sensor, it can be utilized in various applications such as knee rehabilitation assessment, where a highly deformable and a portable measurement system is required.

We first provide an FEM analysis for both EMG and TENG components. Furthermore, a discussion is provided for the configuration of the magnet based on the magnetization direction of the PMs. In addition, we investigate effectiveness of a stack of magnets and coils in a singular package for energy harvesting. The tube based self-powered sensor is then experimentally probed to evaluate its effectiveness for both energy harvesting as well as self-powered sensing. The system is then examined as a cantilever beam which contains two power generation parts. Exerting a periodic deformation to the end of the tube based self-powered sensor triggers both mechanisms of energy harvesting in the proposed system. The proposed self-powered sensor has the potential for knee rehabilitation, as it is flexible, and can be triggered by a bending load. For example, it can be installed in a knee brace for monitoring the health condition of patient's knees.

2. Design

This section illustrates the design components of the proposed hybridized sensory system. The proposed hybridized design integrates electromagnetism and triboelectricity in a single package. Integration of the two energy harvesting mechanisms provides many advantages such as high sensitivity to both small deflection and low frequency. The main structure of the device consists of a flexible tube, round wood, and Viton rubber. Two clamps are used to hold the wood inside of the flexible tube. In our design, we fist consider a single stack of magnet and coil, which consist of two magnets and one coil in the middle of the tube. A flexible foam is located between each set of coil and magnet. In order to increase the capability of our sensing device, we fabricate a larger stack,which includes two coils and three magnets as shown in Figure 1. Section 2.1 demonstrates the configuration and working mechanism of the EMG component considering both single and double stacks in detail. Figure 1 (a) schematically represents the sensing device. Figure 1 (b) shows the zoomed view of the device. Figure 1(c) schematically depicts the device when it is mechanically triggered. When the sensor is deformed as presented in Figure 1 (c), both EMG and TENG components of the sensor are being triggered leading to electricity generation.

Figure 1 (d) shows the zoomed view of the deformed sensor. The TENG component of the sensor includes a layer of Polyurethane attached to the middle of Viton rubber, and also, a layer of Kapton, which is attached to the outer surface of the tube. The two edges of the Viton rubber are attached to the outer surface of the flexible tube as shown in Figure 1(b). The working mechanism and details about the structure of TENG components are provided in Section 2.2. Figure 1(e) shows the fabricated sensor with a single stack EMG component. Figure 1(f) shows as-fabricated sensor with a double stack EMG component incorporated with the TENG component.

2.1. EMG Structure and Working Mechanism

EMG component of the device, as represented in Figure 2, consists of coils, magnets,iron cores, and foams. In a single stack EMG component, as represented in Figure 2(a), the device

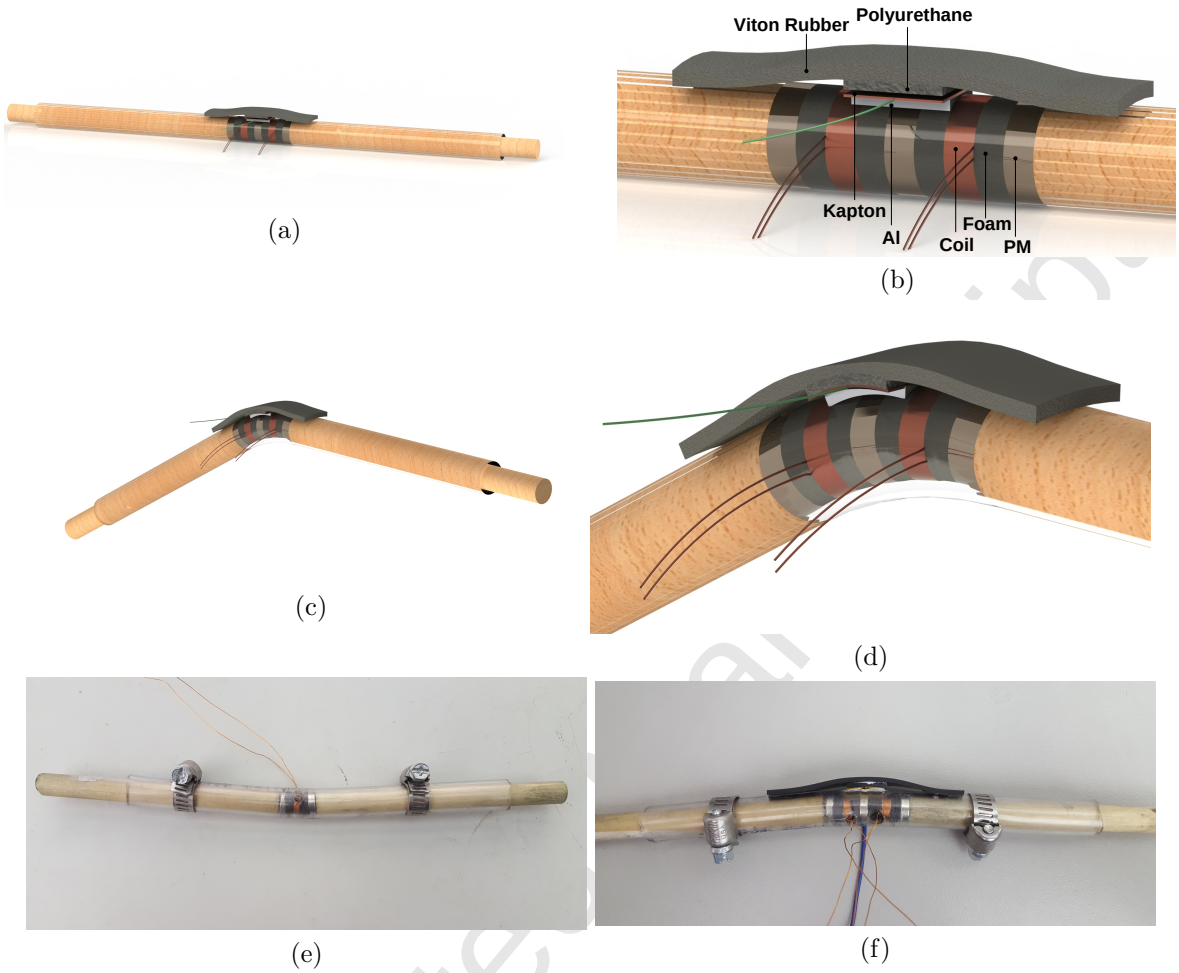

Figure 1: Schematic of the proposed hybrid electromagnetic-triboelectric generator (a) straight tube (b) zoomed view, (c) curved tube (d) zoomed view of the device under deformation; fabricated hybrid electromagnetic-triboelectric generator: (e) single stack (f) double stack.

contains two magnets in left and right sides of a coil equipped by an iron core. Information pertinent to the size of the coils, magnets,and iron cores are provided in Table 1. Coils and magnets are connected to each other through the foam. Foams are glued to the coils and magnets. Figure 2(a) represents coils, magnets,and iron cores of a double stacks self-powered sensing device. Figure 2(b) shows the connected double stacks EMG component of the hybridized device.

When a periodical load is applied to the tip of the sensor,the flexible tube is deformed. Deformation of the flexible tube is transferred to the EMG component through the inner liner of the tube and also two holding woods. Thus, it results in deformation in flexible foam as indicated in Figure 3. The deformation of the flexible foam provides a relative motion between the coils and magnets. Accordingly,electrical current and voltage are generated in coil wires. Direction of the PM magnetization and their configuration selecting procedure are discussed in Section 3.1.

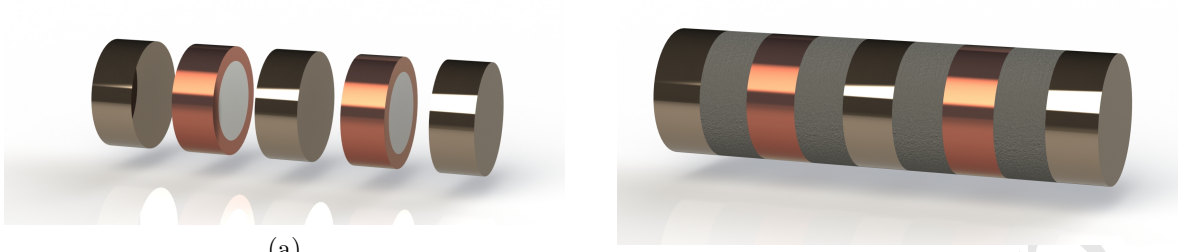

(a) (b)

Figure 2: Electromagnetic component of the sensor (a) without connecting foam (b) with connecting foam.

Table 1: Geometry of the magnets, coils and iron cores

Components	**Thickness**	**Size**	**Turns**	B_r	**AWG**
Round Coil	4 mm	R=1 cm	73	◯	30
Round PM	1/8 in	R=3/8 in	◯	1.35 T	◯
Round core	4 mm	R=6.35 mm	◯	◯	◯

2.2. TENG Structure and Working Mechanism

The operation principle of the TENG sensor is based on the single-electrode mode TENG, as schematically shown in Figure 4 [60]. This part includes highly flexible, mechanically and thermally durable, and cost-effective polymeric materials. When the tube structure is being excited, the contact layers of the TENG sensor will be under contact and separation in each cycle of excitation. When the two layers are in full contact and due to triboelectricity, negative and positive charges are generated in Kapton and Polyurethane surfaces, respectively (Figure 4(a)). The electrode is connected to the electrical ground and no electron flow occurs in between owing to the balance condition. As the two layers separate and a gap takes place, electrons flow from the metal electrode toward the ground due to the variation of local electrical field (Figure 4(b)). The flow continues until reaching the maximum gap where the balance condition is achieved and the charge transfer is stopped (Figure 4(c)). By approaching the Polyurethane layer toward the Kapton layer, the electrons flow back in opposite direction of the separation case (Figure 4(d)).Thus, an alternative current is generated owing to the flow of electrons, which reveals the process of electricity generation.

3. Modelling and EMG Configuration

An important part of the design of the proposed flexible sensor is the magnetization direction of each magnet inside of the tube. We studied the strength of the magnetic field after locating each magnet beside each other using COMSOL, and finally obtained the configuration indicated in Figure 5 as the optimized arrangement for the permanent magnets. Figure 5 represents the implemented arrangement of the PMs and coils in the tube for a simple case, which includes one PM and one coil, a single stack, which contains two PMs and one coil in the middle, and finally, a double stack with three PMs and two

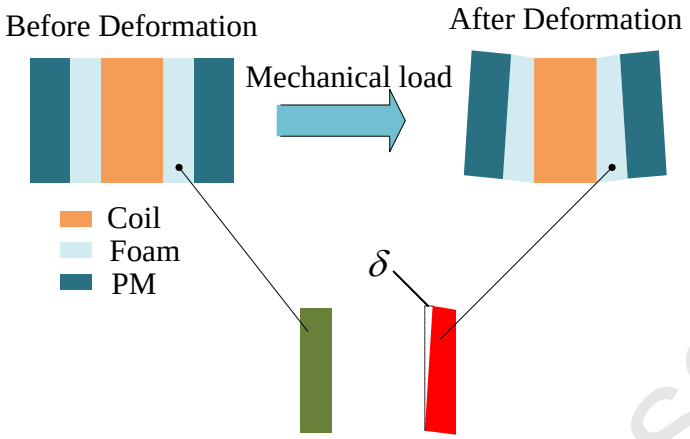

Figure 3: A single stack of EMG component, before and after applying mechanical load to the flexible tube.

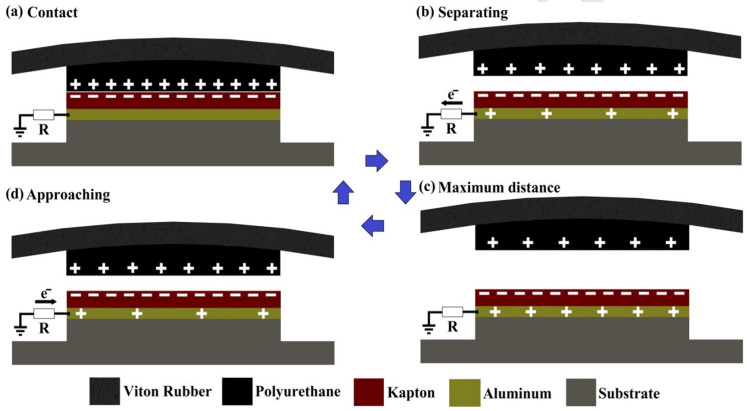

Figure 4: Working mechanism of the single-electrode mode TENG sensor in once full cycle.

coils.Figure 6 shows the curved tube after applying a mechanical load, which results in angle θ. Based on Figure, the angle θ is approximately found by the following simple mathematical calculation:

$$\theta = tan^{-1}\frac{c}{b} \tag{1}$$

This shows that the potential of the device for the angle sensing as will be illustrated in Discussion and Results section. Accordingly, it can be implemented for biomedical applications such as knee rehabilitation. Thus, the sensor can be attached to a knee joint to evaluate the rehabilitation progress of a patient based on the obtained signals through the sensor. Also, with embedding the sensor into the knee brace, the embedded self-powered system can be easily implemented even for rehabilitation exercise at home.

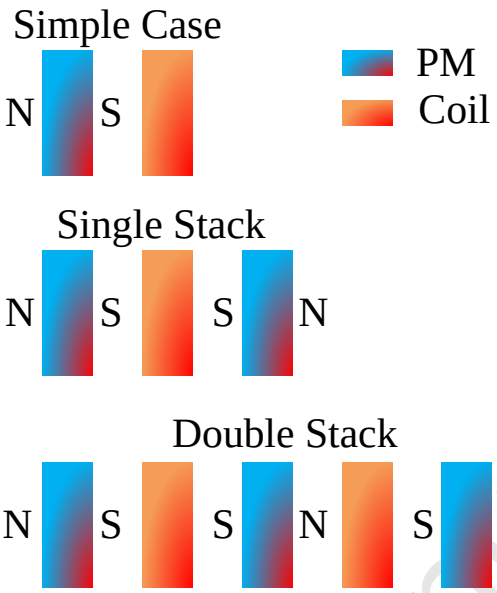

Figure 5: Configuration of the EMG component considering simple case, single stack and double stack of PMs and coils.

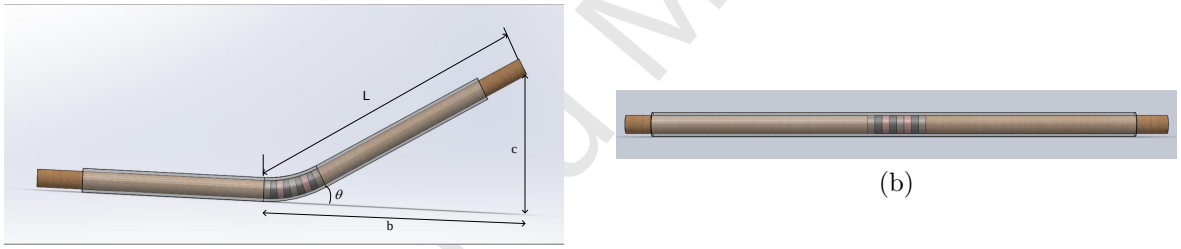

(a) (b)

Figure 6: Self-powered sensor (a) before applying the mechanical load, (b) after applying the mechanical load.

4. Finite Element Analysis

This section presents the Finite element analysis for both EMG and TENG components. Figure 7 represents the FEM results for the EMG components. Figure 7(a) represent the magnetic flux density for a simple system consisting a PM, a coil and an iron core. Figure 7(b) shows the magnetic flux density for a simple system consisting a PM, a coil with air core. Figure 7(c) represents the magnetic flux density for a single stack system without iron core, and Figure 7(d) shows the magnetic flux density for a single stack with iron core. Figures 7(e)-(f) illustrate the magnetic flux density for a double stack system without and with iron cores, respectively. As indicated by the figures, adding iron core to the coil results in enhancement of the magnetic flux density in the coil.

In addition, a study has been performed using finite element method (FEM) to realize

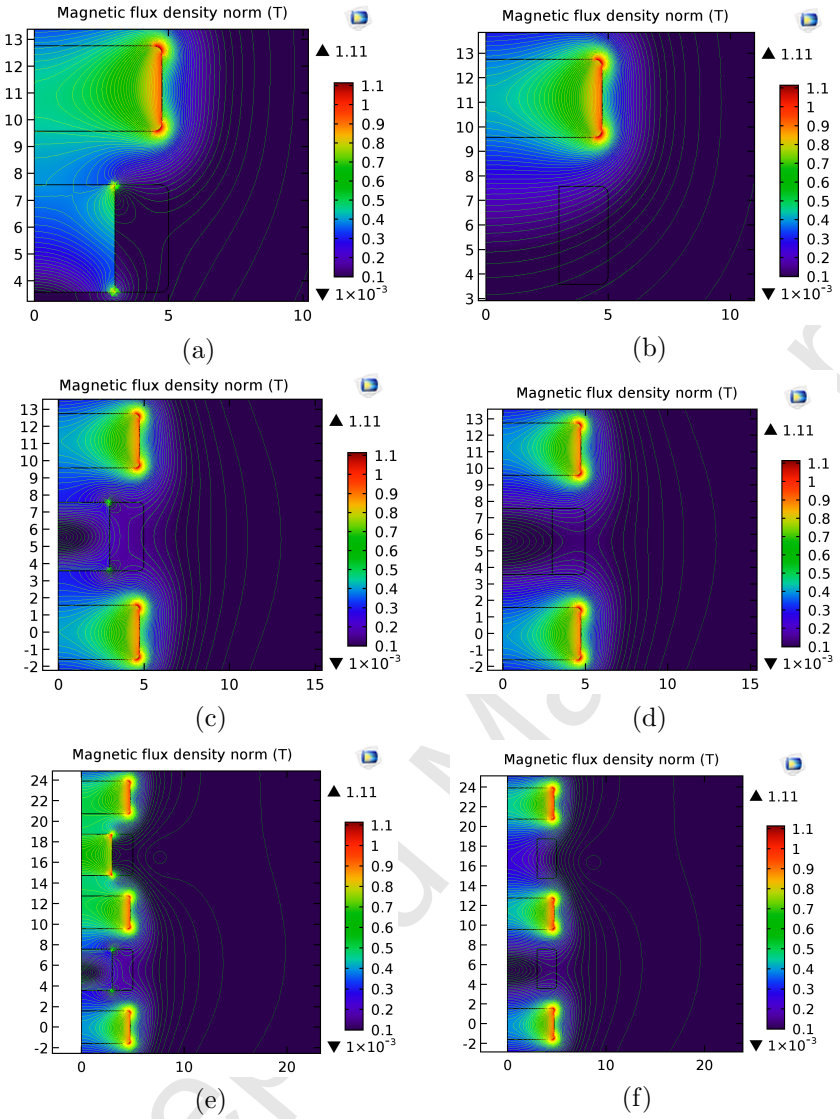

Figure 7: FEM model of the EMG component (a)simple case with iron core, (b) simple case without iron core, (c) single stack with iron core, (d) single stack without iron core, (e) double stack with iron core, (f) double stack without iron core.

the electric potential distribution in the sensor and the charge transfer between the ground and the electrode for the TENG component of the device. Figure 8(a) shows the schematic FEM model developed in COMSOL software in which the effect of changing the relative gap distance, i.e. z, was evaluated. A 2D model was considered since the thickness of contact layers and gaps are relatively small compared to the other dimensions of the device. As Kapton and Polyurethane are insulating materials, charges are uniformly distributed on the contact surfaces. Thus, the Kapton surface was assigned with a charge density of 10 NC/m^2 while a same magnitude with opposite polarity was assign to the Polyurethane surface to maintain the charge conservation. The dimensions were all selected equal to the fabricated

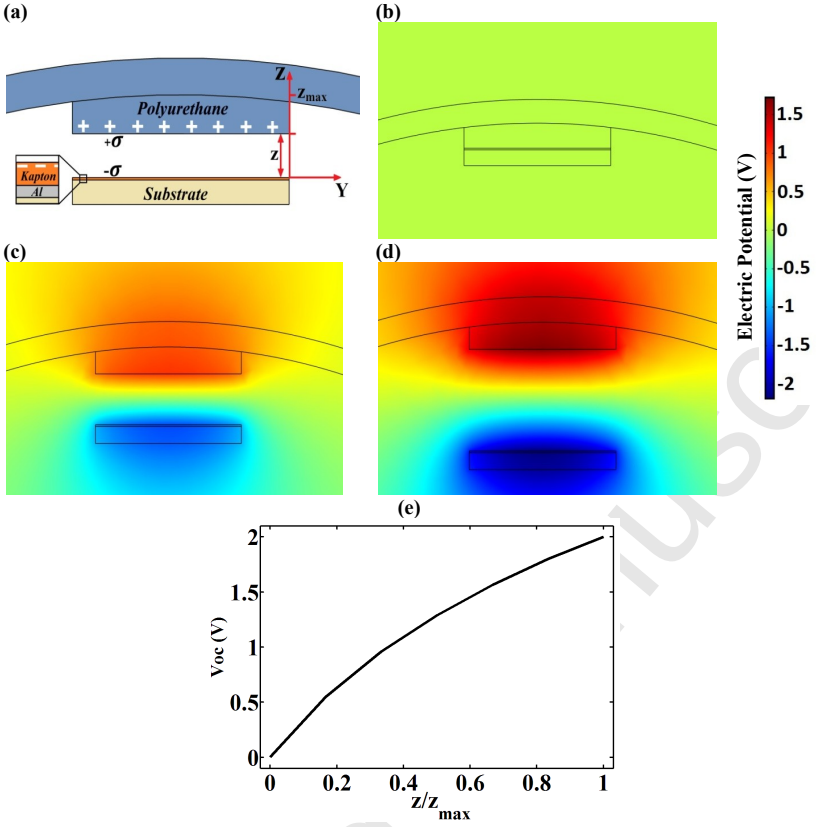

Figure 8: (a) FEA model of the TENG section. (b)-(d) Electric potential distribution for $\frac{z}{z_{max}} = 0, 0.5, 1$ (f) Variation of open-circuit voltage on the electrode versus the relative displacement $\frac{z}{z_{max}}$.

sensor. The model was surrounded by air similar to the actual device and infinity was chosen as the reference point in the simulation. The effect of varying gap on the electric potential distribution was calculated in open-circuit condition. As a result, increasing the gap will enhance the electric potential, as shown in Figures 8(b)-8(d). Also, the variation of open-circuit voltage on the electrode versus the gap distance was shown in Figure 8(e) where the voltage is relatively dependent to the gap size. Therefore, the FEM analysis verifies the process of electricity generation in an excitation cycle where the distance between contact surfaces is being changed from zero to a maximum value.

5. Discussion and Results

This section provides the experimental results and detailed illustration about sensor outputs. Figure 9(a) shows the open circuit voltage of the EMG component for a single stack device. As the figure shows, by increasing the frequency of excitation from 0.5 Hz to 10 Hz, the open circuit voltage increases from 0.2 mV to approximately 1.5 mV. Figure 9(b) represents the sensitivity of the system to the angular amplitude of oscillations. As indicated by the figure, increasing the angular amplitude of excitation at the tip of the sensor, increases

the open circuit voltage. In Figure 9(b) , we converted the shaker's amplitude of excitation to angular deformation based on Figure 6. As the figure shows, the fabricated device is highly sensitive to the angular motion, and a very small angular change results in voltage generation in EMG component. Figure 9(c) illustrates the effect of external resistive load

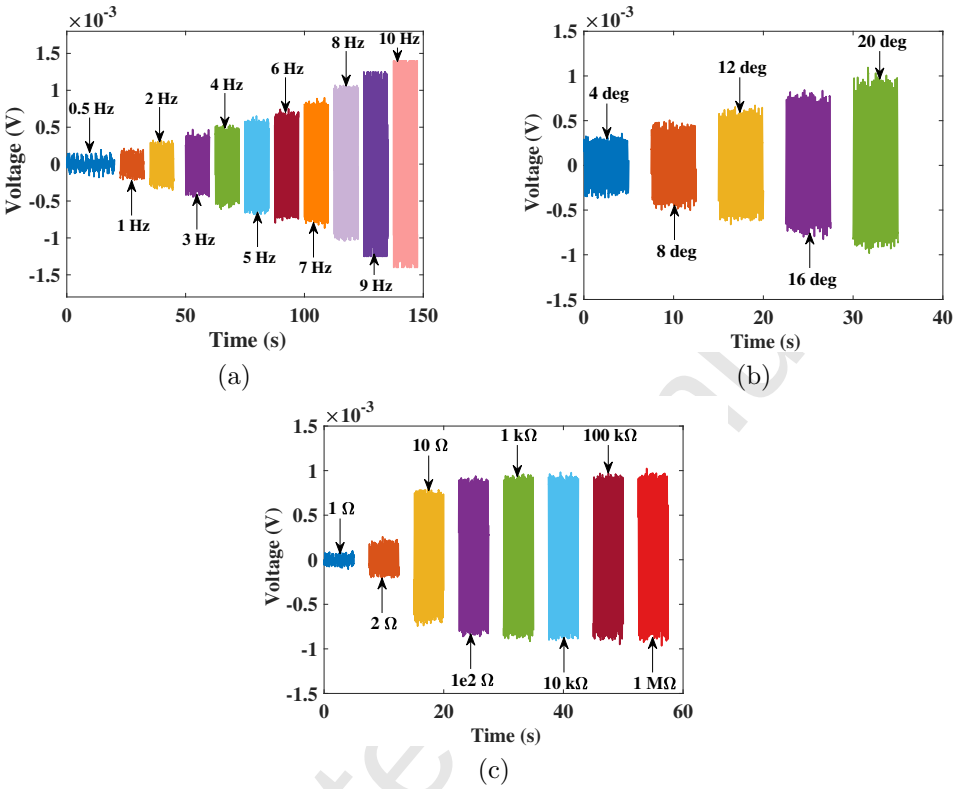

Figure 9: Open circuit voltage of the EMG component-Single Stack (a) effect of triggering frequency (b) effect of angular amplitude of excitation, ($\theta = 4, 8, 12, 16, 20$ degrees) (c) effect of resistive load on the open circuit voltage.

on the EMG component of the single stack device. As expected, increasing the external resistive load enhances the open circuit voltage.

We also studied the electrical output of the system with a double stack EMG component. Figure 10(a) illustrates the influence of the amplitude of excitation on open circuit voltage of the left coil of the double stack EMG component of the sensor. Figure 10(b) represents the effect of the angular amplitude of excitation on open circuit voltage for the right coil of the double stack EMG component. Enhancing the angular amplitude of excitation, increases the open circuit voltage of the both coils. As evidenced by both figures, the highest open circuit voltage for the left coil is approximately 2 mV, and 1.5 mV for the right coil. Accordingly, a double stack of the EMG component can generate approximately 3.5 mV. A single stack of EMG component of the device can approximately deliver 1 mV open circuit voltage as depicted in Figure 9(b). It shows that adding one magnet and one coil to a single stack EMG component and creating a double stack system results in increasing 250 % in the electrical

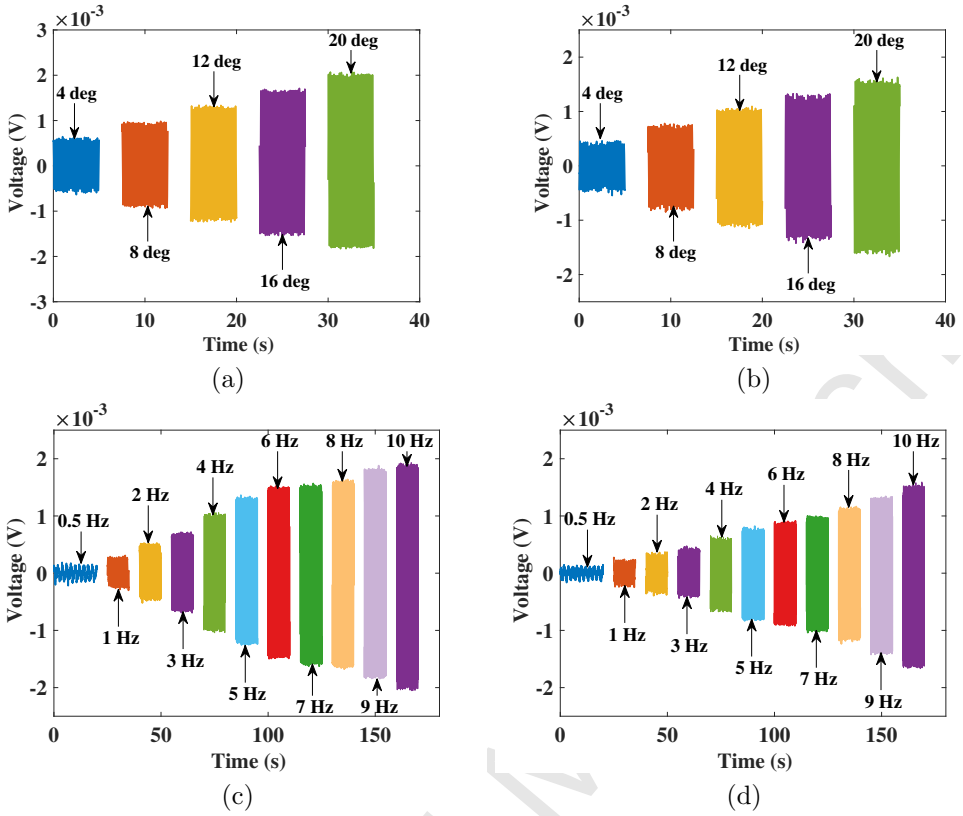

Figure 10: Effect of angular amplitude of excitation on open circuit voltage of the EMG component-Double Stack for ($\theta = 4, 8, 12, 16, 20$ degrees) (a) Left coil (b) Right coil; Effect of triggering frequency on open circuit voltage of the EMG component-Double Stack (c) Left coil (d) Right coil.

output. Figure 10(c) presents the effect of excitation frequency on the open circuit voltage of the left coil.As the figure shows, increasing the excitation frequency from 0.5 Hz to 10 Hz results in increasing approximately 0.15 mV to 1.9 mV. Similarly, Figure 10(d) shows the influence of excitation frequency on the open circuit voltage of the right coil. As expected, increasing the frequency of excitation results in enhancing the open circuit voltage.

Figure 11(a) describes the effect of external resistive load on the output voltage of the TENG component of the device. As expected, by increasing the resistive load, the output voltage of the device increases to reach its open circuit voltage. Figure 11(c) illustrates the effect of angular amplitude of excitation on open circuit voltage of TENG component of the fabricated device. The angular amplitude of excitation varies between 4 to 25 degrees. As depicted by figure, increasing the angular amplitude enhances the open circuit voltage of the TENG component.

In order to further clarify the output performance of the TENG device, the open circuit voltage, transferred charge, and shirt circuit current were evaluated for some special case studies.Figure 12 represents the effect of amplitude of oscillations on the electrical performance of the TENG component of the device. As Figure 12 shows, increasing the angular amplitude of oscillations results in increasing open circuit voltage, transferred charge, and

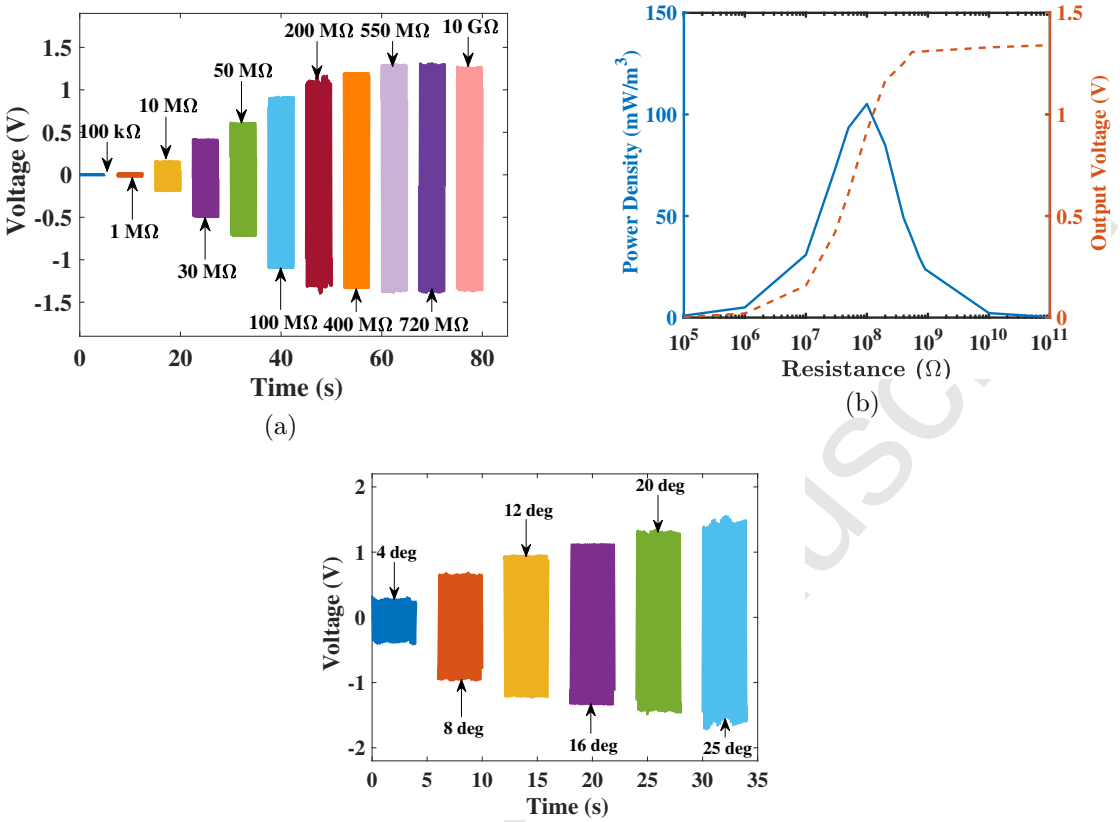

Figure 11: Electrical output of the TENG components, (a)Effect of resistive loads on open circuit voltage between 10^5 to $10^{10}\Omega$, b) Output power and open circuit voltage versus resistive loads, (c) Effect of angular excitations ($\theta = 4, 8, 12, 16, 20, 25$ degrees) on TENG performance.

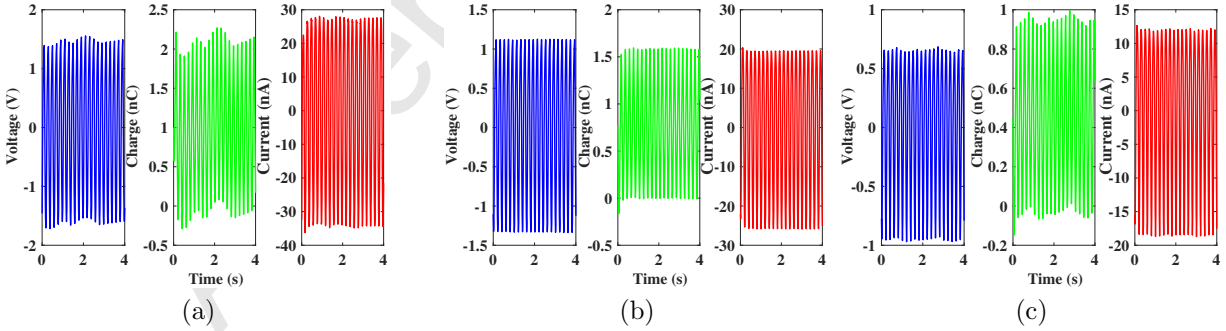

Figure 12: Open circuit voltage of the TENG component (a)angular amplitude,$\theta = 25$ degrees, (b) angular amplitude, $\theta = 16$ degrees,and (c) angular amplitude of oscillation $\theta = 8$ degrees.

short circuit current. Figure 12(a) and (c) represents electrical output pertinent to the highest and lowest amplitude of oscillations, respectively.

To compare the performance of the individual TENG and EMG units with the hybrid

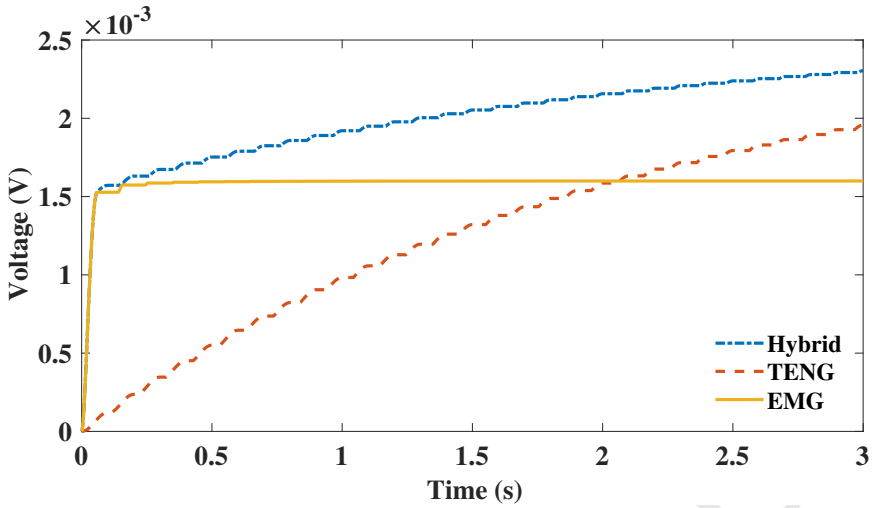

Figure 13: Charging voltage curves for a 10 μF capacitor at 5 Hz excitation using the TENG, EMG and hybrid system.

TENG-EMG system, the performance of the device was evaluated for charging a 10 μF capacitor at a typical frequency i.e. 5 Hz, as shown in Figure 13. The voltage due to individual EMG unit increases promptly up to a specific value where the voltage is then saturated. The voltage of individual TENG increases gradually with a relatively low speed. It is evident that the hybrid system not only reaches to a larger value of voltage than the two individual units, but also shows a faster charging performance which reveals that the performance of hybrid system is superior to each individual TENG and EMG units.

6. Conclusion

We have developed a new type of self-powered sensory device with potential application in vibration/deflection monitoring. The device proposes a hybridized system consists of an electromagnetic and a TENG components. The fabricated system is flexible enough to be implemented for detection of very small angular motions and vibrations. The configuration of the electromagnetic component was optimized with respect to the magnetization direction. In addition, we illustrated how changing the configuration of the electromagnetic component alters the electrical output of the device. The present results show the high sensitivity of the device to a very small angular deflection. This feature of the fabricated device makes it as a suitable candidate for knee rehabilitation evaluation, as it can be embedded into a knee brace.

[1] L. Van Atta, D. Northrup, C. Van Atta, R. Van de Graaff, The design, operation, and performance of the round hill electrostatic generator, Physical review 49 (10) (1936) 761.
[2] R. Herb, D. Parkinson, D. Kerst, The development and performance of an electrostatic generator operating under high air pressure, Physical review 51 (2) (1937) 75.
[3] Z. L. Wang, J. Song, Piezoelectric nanogenerators based on zinc oxide nanowire arrays, Science 312 (5771) (2006) 242–246.

[4] X. Wang, J. Song, J. Liu, Z. L. Wang, Direct-current nanogenerator driven by ultrasonic waves, Science 316 (5821) (2007) 102–105.
[5] P. Glynne-Jones, M. Tudor, S. Beeby, N. White, An electromagnetic, vibration-powered generator for intelligent sensor systems, Sensors and Actuators A: Physical 110 (1) (2004) 344 – 349, selected Papers from Eurosensors XVI Prague, Czech Republic.
[6] Z. Lin, J. Chen, X. Li, J. Li, J. Liu, Q. Awais, J. Yang, Broadband and three-dimensional vibration energy harvesting by a non-linear magnetoelectric generator, Applied Physics Letters 109 (25) (2016) 253903.
[7] Z. L. Wang, J. Chen, L. Lin, Progress in triboelectric nanogenerators as a new energy technology and self-powered sensors, Energy & Environmental Science 8 (8) (2015) 2250–2282.
[8] J. Chen, Z. L. Wang, Reviving vibration energy harvesting and self-powered sensing by a triboelectric nanogenerator, Joule 1 (2017) 480–521.
[9] J. Chen, Y. Huang, N. Zhang, H. Zou, R. Liu, C. Tao, X. Fan, Z. L. Wang, Micro-cable structured textile for simultaneously harvesting solar and mechanical energy, Nature Energy 1 (10) (2016) 16138.
[10] G. Zhu, J. Chen, T. Zhang, Q. Jing, Z. L. Wang, Radial-arrayed rotary electrification for high performance triboelectric generator, Nature communications 5 (2014) 3426.
[11] G. Zhu, Y. S. Zhou, P. Bai, X. S. Meng, Q. Jing, J. Chen, Z. L. Wang, A shape-adaptive thin-film-based approach for 50 % high-efficiency energy generation through micro-grating sliding electrification, Advanced Materials 26 (23) (2014) 3788–3796.
[12] G. Zhu, P. Bai, J. Chen, Z. L. Wang, Power-generating shoe insole based on triboelectric nanogenerators for self-powered consumer electronics, Nano Energy 2 (5) (2013) 688 – 692.
[13] J. Chen, G. Zhu, J. Yang, Q. Jing, P. Bai, W. Yang, X. Qi, Y. Su, Z. L. Wang, Personalized keystroke dynamics for self-powered humanmachine interfacing, ACS Nano 9 (1) (2015) 105–116.
[14] L. Zheng, G. Cheng, J. Chen, L. Lin, J. Wang, Y. Liu, H. Li, Z. L. Wang, A hybridized power panel to simultaneously generate electricity from sunlight, raindrops, and wind around the clock, Advanced Energy Materials 5 (21) (2015) 1501152.
[15] Z. Lin, J. Chen, X. Li, Z. Zhou, K. Meng, W. Wei, J. Yang, Z. L. Wang, Triboelectric nanogenerator enabled body sensor network for self-powered human heart-rate monitoring, ACS Nano 11 (9) (2017) 8830–8837.
[16] W. Yang, J. Chen, X. Wen, Q. Jing, J. Yang, Y. Su, G. Zhu, W. Wu, Z. L. Wang, Triboelectrification based motion sensor for human-machine interfacing, ACS Applied Materials & Interfaces 6 (10) (2014) 7479–7484.
[17] B. Zhang, J. Chen, L. Jin, W. Deng, L. Zhang, H. Zhang, M. Zhu, W. Yang, Z. L. Wang, Rotating-disk-based hybridized electromagnetictriboelectric nanogenerator for sustainably powering wireless traffic volume sensors, ACS Nano 10 (6) (2016) 6241–6247.
[18] J. Chen, J. Yang, H. Guo, Z. Li, L. Zheng, Y. Su, Z. Wen, X. Fan, Z. L. Wang, Automatic mode transition enabled robust triboelectric nanogenerators, ACS Nano 9 (12) (2015) 12334–12343.
[19] Z. Saadatnia, E. Asadi, H. Askari, J. Zu, E. Esmailzadeh, Modeling and performance analysis of duck-shaped triboelectric and electromagnetic generators for water wave energy harvesting, International Journal of Energy Research 41 (14) (2017) 2392–2404.
[20] H. Askari, E. Asadi, Z. Saadatnia, A. Khajepour, M. B. Khamesee, J. Zu, A hybridized electromagnetic-triboelectric self-powered sensor for traffic monitoring: concept, modelling, and optimization, Nano Energy 32 (2017) 105 – 116.
[21] Y. Yang, H. Zhang, Z.-H. Lin, Y. S. Zhou, Q. Jing, Y. Su, J. Yang, J. Chen, C. Hu, Z. L. Wang, Human skin based triboelectric nanogenerators for harvesting biomechanical energy and as self-powered active tactile sensor system, ACS nano 7 (10) (2013) 9213–9222.
[22] L. Zhang, B. Zhang, J. Chen, L. Jin, W. Deng, J. Tang, H. Zhang, H. Pan, M. Zhu, W. Yang, Z. L. Wang, Lawn structured triboelectric nanogenerators for scavenging sweeping wind energy on rooftops, Advanced Materials 28 (8) (2016) 1650–1656.
[23] P. Bai, G. Zhu, Q. Jing, Y. Wu, J. Yang, J. Chen, J. Ma, G. Zhang, Z. L. Wang, Transparent and flexible barcode based on sliding electrification for self-powered identification systems, Nano Energy 12

(2015) 278 – 286.

[24] Z. Wen, J. Chen, M.-H. Yeh, H. Guo, Z. Li, X. Fan, T. Zhang, L. Zhu, Z. L. Wang, Blow-driven triboelectric nanogenerator as an active alcohol breath analyzer, Nano Energy 16 (2015) 38 – 46.

[25] G. Zhu, Y. Su, P. Bai, J. Chen, Q. Jing, W. Yang, Z. L. Wang, Harvesting water wave energy by asymmetric screening of electrostatic charges on a nanostructured hydrophobic thin-film surface, ACS Nano 8 (6) (2014) 6031–6037.

[26] Y. Su, X. Wen, G. Zhu, J. Yang, J. Chen, P. Bai, Z. Wu, Y. Jiang, Z. L. Wang, Hybrid triboelectric nanogenerator for harvesting water wave energy and as a self-powered distress signal emitter, Nano Energy 9 (2014) 186 – 195.

[27] B. J. Kim, D. H. Kim, Y.-Y. Lee, H.-W. Shin, G. S. Han, J. S. Hong, K. Mahmood, T. K. Ahn, Y.-C. Joo, K. S. Hong, et al., Highly efficient and bending durable perovskite solar cells: toward a wearable power source, Energy & Environmental Science 8 (3) (2015) 916–921.

[28] Z. Li, J. Chen, H. Guo, X. Fan, Z. Wen, M.-H. Yeh, C. Yu, X. Cao, Z. L. Wang, Triboelectrification-enabled self-powered detection and removal of heavy metal ions in wastewater, Advanced Materials 28 (15) (2016) 2983–2991.

[29] J. Chen, G. Zhu, W. Yang, Q. Jing, P. Bai, Y. Yang, T.-C. Hou, Z. L. Wang, Harmonic-resonator-based triboelectric nanogenerator as a sustainable power source and a self-powered active vibration sensor, Advanced materials 25 (42) (2013) 6094–6099.

[30] W. Yang, J. Chen, Q. Jing, J. Yang, X. Wen, Y. Su, G. Zhu, P. Bai, Z. L. Wang, 3d stack integrated triboelectric nanogenerator for harvesting vibration energy, Advanced Functional Materials 24 (26) (2014) 4090–4096.

[31] W. Yang, J. Chen, G. Zhu, J. Yang, P. Bai, Y. Su, Q. Jing, X. Cao, Z. L. Wang, Harvesting energy from the natural vibration of human walking, ACS nano 7 (12) (2013) 11317–11324.

[32] W. Yang, J. Chen, G. Zhu, X. Wen, P. Bai, Y. Su, Y. Lin, Z. Wang, Harvesting vibration energy by a triple-cantilever based triboelectric nanogenerator, Nano Research 6 (12) (2013) 880–886.

[33] J. Yang, J. Chen, Y. Yang, H. Zhang, W. Yang, P. Bai, Y. Su, Z. L. Wang, Broadband vibrational energy harvesting based on a triboelectric nanogenerator, Advanced Energy Materials 4 (6) (2014) 1301322.

[34] G. Zhu, J. Chen, Y. Liu, P. Bai, Y. S. Zhou, Q. Jing, C. Pan, Z. L. Wang, Linear-grating triboelectric generator based on sliding electrification, Nano letters 13 (5) (2013) 2282–2289.

[35] P. Bai, G. Zhu, Y. Liu, J. Chen, Q. Jing, W. Yang, J. Ma, G. Zhang, Z. L. Wang, Cylindrical rotating triboelectric nanogenerator, ACS nano 7 (7) (2013) 6361–6366.

[36] Q. Jing, G. Zhu, P. Bai, Y. Xie, J. Chen, R. P. Han, Z. L. Wang, Case-encapsulated triboelectric nanogenerator for harvesting energy from reciprocating sliding motion, ACS nano 8 (4) (2014) 3836–3842.

[37] S. Y. Kuang, J. Chen, X. B. Cheng, G. Zhu, Z. L. Wang, Two-dimensional rotary triboelectric nanogenerator as a portable and wearable power source for electronics, Nano Energy 17 (2015) 10 – 16.

[38] Y. Yang, H. Zhang, J. Chen, Q. Jing, Y. S. Zhou, X. Wen, Z. L. Wang, Single-electrode-based sliding triboelectric nanogenerator for self-powered displacement vector sensor system, Acs Nano 7 (8) (2013) 7342–7351.

[39] J. Yang, J. Chen, Y. Su, Q. Jing, Z. Li, F. Yi, X. Wen, Z. Wang, Z. L. Wang, Eardrum-inspired active sensors for self-powered cardiovascular system characterization and throat-attached anti-interference voice recognition, Advanced Materials 27 (8) (2015) 1316–1326.

[40] Y. Yang, G. Zhu, H. Zhang, J. Chen, X. Zhong, Z.-H. Lin, Y. Su, P. Bai, X. Wen, Z. L. Wang, Triboelectric nanogenerator for harvesting wind energy and as self-powered wind vector sensor system, ACS nano 7 (10) (2013) 9461–9468.

[41] Y. Su, G. Zhu, W. Yang, J. Yang, J. Chen, Q. Jing, Z. Wu, Y. Jiang, Z. L. Wang, Triboelectric sensor for self-powered tracking of object motion inside tubing, ACS nano 8 (4) (2014) 3843–3850.

[42] S. Wang, Y. Xie, S. Niu, L. Lin, Z. L. Wang, Freestanding triboelectric-layer-based nanogenerators for harvesting energy from a moving object or human motion in contact and non-contact modes, Advanced Materials 26 (18) (2014) 2818–2824.

[43] H. Guo, J. Chen, M.-H. Yeh, X. Fan, Z. Wen, Z. Li, C. Hu, Z. L. Wang, An ultrarobust high-performance triboelectric nanogenerator based on charge replenishment, ACS nano 9 (5) (2015) 5577–5584.
[44] S. Wang, L. Lin, Z. L. Wang, Nanoscale triboelectric-effect-enabled energy conversion for sustainably powering portable electronics, Nano Letters 12 (12) (2012) 6339–6346.
[45] G. Zhu, C. Pan, W. Guo, C.-Y. Chen, Y. Zhou, R. Yu, Z. L. Wang, Triboelectric-generator-driven pulse electrodeposition for micropatterning, Nano Letters 12 (9) (2012) 4960–4965.
[46] G. Cheng, Z.-H. Lin, L. Lin, Z.-l. Du, Z. L. Wang, Pulsed nanogenerator with huge instantaneous output power density, ACS Nano 7 (8) (2013) 7383–7391.
[47] X. He, H. Guo, X. Yue, J. Gao, Y. Xi, C. Hu, Improving energy conversion efficiency for triboelectric nanogenerator with capacitor structure by maximizing surface charge density, Nanoscale 7 (5) (2015) 1896–1903.
[48] T. Jiang, Y. Yao, L. Xu, L. Zhang, T. Xiao, Z. L. Wang, Spring-assisted triboelectric nanogenerator for efficiently harvesting water wave energy, Nano Energy 31 (2017) 560 – 567.
[49] U. Khan, S.-W. Kim, Triboelectric nanogenerators for blue energy harvesting, ACS Nano 10 (7) (2016) 6429–6432.
[50] J. Bae, J. Lee, S. Kim, J. Ha, B.-S. Lee, Y. Park, C. Choong, J.-B. Kim, Z. L. Wang, H.-Y. Kim, et al., Flutter-driven triboelectrification for harvesting wind energy, Nature communications 5 (2014) 4929.
[51] J. Chen, J. Yang, Z. Li, X. Fan, Y. Zi, Q. Jing, H. Guo, Z. Wen, K. C. Pradel, S. Niu, Z. L. Wang, Networks of triboelectric nanogenerators for harvesting water wave energy: A potential approach toward blue energy, ACS Nano 9 (3) (2015) 3324–3331.
[52] F.-R. Fan, L. Lin, G. Zhu, W. Wu, R. Zhang, Z. L. Wang, Transparent triboelectric nanogenerators and self-powered pressure sensors based on micropatterned plastic films, Nano Letters 12 (6) (2012) 3109–3114.
[53] L. Dhakar, S. Gudla, X. Shan, Z. Wang, F. E. H. Tay, C.-H. Heng, C. Lee, Large scale triboelectric nanogenerator and self-powered pressure sensor array using low cost roll-to-roll uv embossing, Scientific reports 6 (2016) 22253.
[54] K. Y. Lee, H.-J. Yoon, T. Jiang, X. Wen, W. Seung, S.-W. Kim, Z. L. Wang, Fully packaged self-powered triboelectric pressure sensor using hemispheres-array, Advanced Energy Materials 6 (11) (2016) 1502566.
[55] R. Hinchet, S.-W. Kim, Wearable and implantable mechanical energy harvesters for self-powered biomedical systems, ACS Nano 9 (8) (2015) 7742–7745.
[56] J. Wang, S. Li, F. Yi, Y. Zi, J. Lin, X. Wang, Y. Xu, Z. L. Wang, Sustainably powering wearable electronics solely by biomechanical energy, Nature communications 7.
[57] W. Tang, J. Tian, Q. Zheng, L. Yan, J. Wang, Z. Li, Z. L. Wang, Implantable self-powered low-level laser cure system for mouse embryonic osteoblasts proliferation and differentiation, ACS Nano 9 (8) (2015) 7867–7873.
[58] S. Li, W. Peng, J. Wang, L. Lin, Y. Zi, G. Zhang, Z. L. Wang, All-elastomer-based triboelectric nanogenerator as a keyboard cover to harvest typing energy, ACS Nano 10 (8) (2016) 7973–7981.
[59] A. Ahmed, S. L. Zhang, I. Hassan, Z. Saadatnia, Y. Zi, J. Zu, Z. L. Wang, A washable, stretchable, and self-powered human-machine interfacing triboelectric nanogenerator for wireless communications and soft robotics pressure sensor arrays, Extreme Mechanics Letters 13 (2017) 25 – 35.
[60] S. Niu, Y. Liu, S. Wang, L. Lin, Y. S. Zhou, Y. Hu, Z. L. Wang, Theoretical investigation and structural optimization of single-electrode triboelectric nanogenerators, Advanced Functional Materials 24 (22) (2014) 3332–3340.

Short Bio

Hassan Askari is a researcher at Mechanical and Mechatronics Engineering Department of University of Waterloo, Waterloo, ON, Canada. He is currently developing new types of self-powered sensors for harsh environment. His area of expertise includes self-powered sensors, nonlinear vibrations, nano structures, and applied mathematics. His research works result in more than 50 papers in refereed well-known journals and conferences.

Zia Saadatniareceived his BSc and MASc degrees from Iran University of Science and Technology and University of Ontario Institute of Technology, respectively. He is currently a PhD Candidate in Mechanical Engineering at University of Toronto, Canada. His current research is mainly focused on Energy harvesting, Self-Powered Sensors and Nonlinear Vibration.

Ehsan Asadireceived his PhD degree from University of Waterloo, ON, Canada M.Sc degree from the School of Mechatronic Systems Engineering at Simon Fraser University, Vancouver, BC, Canada. He is currently a researcher in Mechanical and Mechatronic Engineering department at the University of Waterloo, Waterloo, ON, Canada where he is working toward developing electromagnetic hybrid vibration isolation systems. His area of expertise is design, modelling, and experimental analyses of electromechanical, vibration isolation and dynamic systems. He has successfully applied his skills to applications like electromechanical actuators and vibration isolators, rehabilitation, robotics and haptics.

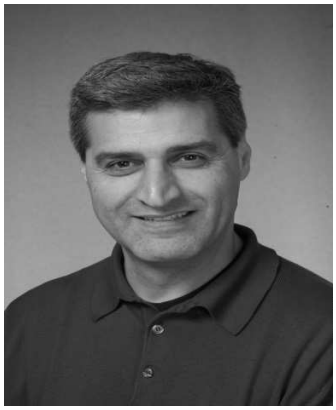

Hassan Askari is a Professor of mechanical and mechatronics engineering with the University of Waterloo, Waterloo, ON, Canada, and the Canada Research Chair in Mechatronic Vehicle Systems. He has developed an extensive research program that applies his expertise in several key multidisciplinary areas. His research interests include modeling and control of dynamic systems. His research has resulted in several patents and technology transfers. He is the author of more than 400 journal and conference publications and five books. He is a Fellow of the Engineering Institute of Canada, the American Society of Mechanical Engineers, and the Canadian Society of Mechanical Engineering.

Mir Behrad Khamesee received the M.S. and Ph.D. degrees from Mie University, Tsu, Japan, in 1996 and 1999, respectively, both in mechanical engineering (mechatronics) and under a Japanese government scholarship.

He worked in industry in Japan from 1999 to 2002. He was a Postdoctoral Fellow with the University of Alberta, Canada, from 2002 to 2003. In March 2004, he became an Assistant Professor at the University of Waterloo, Waterloo, ON, Canada, and he was promoted two times; in July 2009 as an Associate Professor, and in July 2015 as a Professor. Dr. Khamesee is the director of Maglev Microrobotics Laboratory, and his research interests include design, modeling, and control of advanced mechatronics systems, particularly microrobotic magnetic levitation and regenerative electromagnetic shock absorbers.

Dr. Khamesee is involved in conferences program committees, has organized several sessions at international conferences, and is a Technical Reviewer for several Journals.

Jean Zugraduated with B.Sc. in 1984 and M.Sc. in 1986 from Tsinghua University. After two years of working as a lecturer and researcher at Tsinghua University, she came to Canada, and obtained her Ph.D. from the University of Manitoba in 1993. In January 1994, she joined the University of Toronto, Department of Mechanical & Industrial Engineering as an Assistant Professor. She was promoted to Associate Professor in 1999 and to Full Professor in 2004. From June 2008 to June 2009, she served as Associate Chair of Research. She currently serves as Chair of the Department (from July 1, 2009). Her research has been focused on vibration control, dynamics analysis, energy harvesting, and actuators.

Highlight

- A new type of self-powered sensor with applications in angular motion sensing is presented.
- Triboelectric and electromagnetic generators are hybridized in a singular package.
- An optimized configuration is determined for the electromagnetic configuration of the self-powered sensor.
- The potential of the device for joint and knee rehabilitation is discussed.
- Design and modelling of both EMG and TENG parts are fully discussed.